

Critical behaviors of half-metallic ferromagnet $\text{Co}_3\text{Sn}_2\text{S}_2$

Weinian Yan¹, Xiao Zhang^{1,*}, Qi Shi¹, Xiaoyun Yu¹, Zhiqing Zhang¹, Qi Wang², Si Li¹, and Hechang Lei²

¹*State Key Laboratory of Information Photonics and Optical Communications & School of Science, Beijing University of Posts and Telecommunications, Beijing 100876, China*

²*Department of Physics and Beijing Key Laboratory of Opto-electronic Functional Materials & Micro-nano Devices, Renmin University of China, Beijing 100872, China*

(Dated: January 25, 2018)

We have investigated the critical behavior of a shandite-type half-metal ferromagnet $\text{Co}_3\text{Sn}_2\text{S}_2$. It exhibits a second-order paramagnetic-ferromagnetic phase transition with $T_C = 174$ K. To investigate the nature of the magnetic phase transition, a detailed critical exponent study has been performed. The critical components β , γ , and δ determined using the modified Arrott plot, the Kouvel-Fisher method as well as the critical isotherm analysis are match reasonably well and follow the scaling equation, confirming that the exponents are unambiguous and intrinsic to the material. The determined exponents of $\text{Co}_3\text{Sn}_2\text{S}_2$ deviates from theoretical estimated short-range universal models. Instead, $\text{Co}_3\text{Sn}_2\text{S}_2$ exhibits long-range order in the nature of magnetic interaction with the spin decay as $J(r) \sim 1/r^{-(d+\sigma)}$ with $\sigma = 1.28$.

I. INTRODUCTION

The investigation of phase transition in magnetic materials provides insight into the fundamental interactions and the global properties, such as the space dimensionality, the range of interaction, and the symmetry of the order parameter within a given universality class that the critical exponents and scaling functions are identical for all systems.¹⁻⁴ Most of the theories of critical phenomena mainly study the magnets in which the magnetic moments are localized at lattice sites and interacting with one another through exchange interactions. In contrast, experimental studies on the critical behaviors of itinerant ferromagnets (IFMs) near the ferromagnetism (FM) and paramagnetism (PM) phase transition are confined to only a few systems.⁵⁻⁹ Itinerant ferromagnetism is based on the band theory of electrons and the magnetic moment arises from the exchange splitting of the band.^{10,11} Although modern theories developed from the Stoner mean field model can explain well various characteristic physical properties of IFMs,^{10,11} such as Curie temperature (T_C), temperature dependence of spontaneous magnetization, $M(T, 0)$ for $T < T_C$ and Curie-Weiss behavior of susceptibility, $\chi(T)$ when $T > T_C$ etc, they still inadequately explain the critical behaviors of these systems.¹²

Among IFMs, half-metallic ferromagnets (HMFMs) belong to one of limits. In general, they are metals with a Fermi surface in one spin channel but for the other there is a gap in the spin-polarized density of states (DOS), like a semiconductor or insulator.^{13,14} Because of very limited HMFMs reports, such as Heusler alloys,¹³ CrO_2 ,¹⁵ and $\text{Sr}_2\text{FeMoO}_6$,¹⁶ the physical properties of HMFMS are not fully understood, let alone their critical behaviors. On the other hand, the HMFMs are also essential for applications related to magnetism and spintronics.^{17,18} For example, half-metallic ferromagnetic electrodes can be used as ideal spin injectors and detectors, because they can carry current in only one spin direction. They are also important components for giant magnetoresistance

(GMR) and tunneling magnetoresistance (TMR) devices.

Recently, the shandite-type HFM $\text{Co}_3\text{Sn}_2\text{S}_2$ with $T_C = 174$ K has attracted much research attention.¹⁹⁻²² It exhibits large intrinsic anomalous Hall effect, originating from the Weyl fermions near the Fermi energy.^{21,22} More importantly, the density-functional theory (DFT) calculations indicate that a ferromagnetic phase transition in this compound is accompanied by the formation of a band gap in spin minority direction.¹⁹ According to the classification given by Coey,¹⁵ $\text{Co}_3\text{Sn}_2\text{S}_2$ is a type I_A HFM, which is an ideal material for the spintronics devices because of the fully spin polarization at the Fermi energy. Since only very few compounds have been proven to be HMFMs with high T_C , the detailed experimental study on the physical properties of $\text{Co}_3\text{Sn}_2\text{S}_2$ is very important. But the investigations on the critical behaviors of $\text{Co}_3\text{Sn}_2\text{S}_2$ single crystal are still scarce.

In this work, we studied the critical behaviors of $\text{Co}_3\text{Sn}_2\text{S}_2$ single crystal. For the understanding of the nature of magnetic phase transition, we performed a critical exponent analysis in the vicinity of the FM-PM transition region, where the critical exponents have been obtained reliably by different analytical methods. This is an effective way to clarify the magnetic interactions and properties of $\text{Co}_3\text{Sn}_2\text{S}_2$.^{23,24}

II. EXPERIMENTAL

Single crystals of $\text{Co}_3\text{Sn}_2\text{S}_2$ were grown from Sn flux.²⁵ X-ray diffraction (XRD) of well-grounded crystals and a single crystal was performed using a Bruker D8 X-ray diffractometer with Cu K_α radiation ($\lambda = 0.15418$ nm) at room temperature. Rietveld refinements of the data were performed with the TOPAS package.²⁶ Magnetization measurements were carried out using Quantum Design MPMS3.

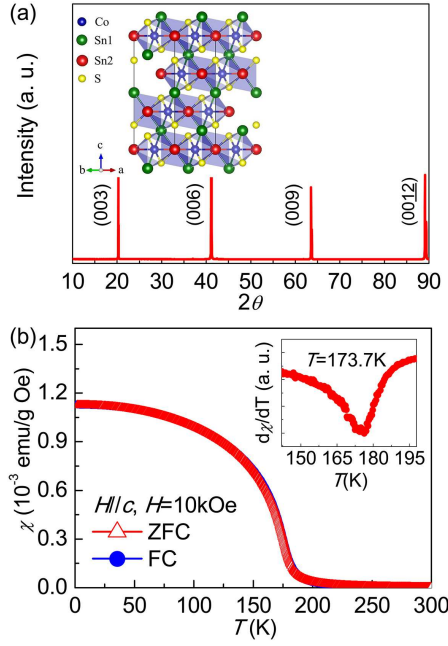


FIG. 1. (a) XRD pattern of a $\text{Co}_3\text{Sn}_2\text{S}_2$ single crystal. Inset: crystal structure of $\text{Co}_3\text{Sn}_2\text{S}_2$ with Co, Sn1, Sn2 and S atoms representing by the blue, green, red and yellow balls, respectively. (b) Temperature dependence of magnetic susceptibility $\chi(T)$ with ZFC and FC modes at $H = 10$ kOe from 2 K to 300 K. Inset: Temperature dependence of $d\chi/dT$.

III. RESULTS AND DISCUSSION

The crystal structure of $\text{Co}_3\text{Sn}_2\text{S}_2$ is shown in the inset of Fig. 1(a). One Co atom is coordinated with four Sn atoms (Sn2 site) and two S atoms, forming a tetragonal bipyramid (distorted octahedron). These octahedra connect each other along ab -plane by face-sharing and along c -axis by corner-sharing. The slabs of CoSn_4S_2 octahedra stack in a hexagonal packing (A-B-C fashion) along c -axis. Another Sn atoms (Sn1 site) are situated in between CoSn_4S_2 slabs, interconnecting them. The XRD pattern of a single crystal can be indexed by the indices of (00l) lattice planes (Fig. 1(a)), indicating that the crystal surface is normal to the c -axis with the plate-shaped surface parallel to the ab plane. Fig. 1(b) shows the temperature dependence of the magnetic susceptibility $\chi(T)$ with the zero-field-cooling (ZFC) and field-cooling (FC) modes at an applied field of 10 kOe, suggesting this system has a ferromagnetic phase transition with $T_C \sim 173.7$ K (defined as the temperature corresponding to the peak of $d\chi/dT$ curve (inset of Fig. 1(b))). It is consistent with previous reports.^{21,27}

Fig. 2(a) displays the isothermal magnetization curves $M(H)$ of $\text{Co}_3\text{Sn}_2\text{S}_2$ measured in the temperature range from 150 K to 200 K with temperature steps of 2 K. The shapes of $M(H)$ curves is typical for ferromagnet. The curves below T_C rise sharply at low-field region and saturate at high-field region. In contrast, when $T > T_C$, the curves gradually become linear. For determining the

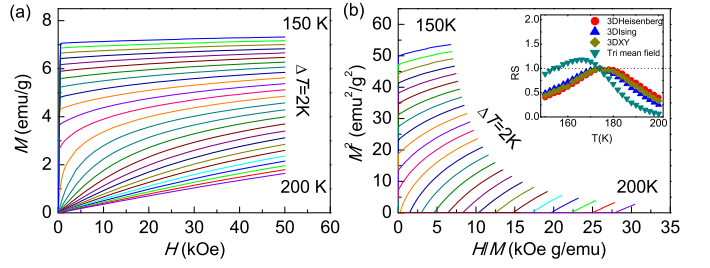


FIG. 2. (a) The initial isothermal magnetization around T_C . (b) Arrott plot with mean field model. Inset: Relative slope (RS) as a function of temperature.

type of magnetic phase transition, we firstly plotted the curves of M^2 vs. H/M , known as the standard Arrott plot (Fig. 2(b)). Based on the criterion,²⁸ the magnetic transition order can be determined from the slope of the standard Arrott plot. The negative slope indicates the first-order transition while the positive slope indicates the second-order one. Apparently, the positive slope of the M^2 vs H/M indicates that $\text{Co}_3\text{Sn}_2\text{S}_2$ undergoes a second-order PM-FM phase transition in the vicinity of T_C . However, in the long-range Landau mean-field theory, the curves of M^2 vs. H/M at various T should form a progression of parallel straight lines in the high-field region with the line at $T = T_C$ passing through the origin. But the Arrott plot presented in Fig. 2(b) are not linear in the high-field region, it implies that the mean-field theory can not describe the critical behavior of $\text{Co}_3\text{Sn}_2\text{S}_2$. Thus, the $M(H)$ results are analyzed according to the Arrot-Noaks equation of state $(H/M)^{1/\gamma} = a\varepsilon + bM^{1/\beta}$, where $\varepsilon = (T - T_C)/T_C$ is the reduced temperature, a and b are coefficients, and the critical exponents β , γ are respectively associated with the spontaneous magnetization $M_s(T) = \lim_{H \rightarrow 0} H$ and inverse initial susceptibility $\chi_0^{-1}(T) = \lim_{H \rightarrow 0} (H/M)$,³²

$$M_S(T, 0) = M_0(-\varepsilon)^\beta, \varepsilon < 0, T < T_C \quad (1)$$

$$\chi_0^{-1}(T) = (h_0/M_0)\varepsilon^\gamma, \varepsilon > 0, T > T_C \quad (2)$$

where M_0 , and h_0/M_0 are the critical amplitudes. Correct values of β and γ will lead to a bunch of parallel straight lines of $M^{1/\beta}$ vs. $(H/M)^{1/\gamma}$ at various temperatures. Moreover, the line at $T = T_c$ should pass through the origin. Using the critical exponents of 3D Heisenberg model ($\beta = 0.365$ and $\gamma = 1.336$), 3D Ising model ($\beta = 0.325$ and $\gamma = 1.24$), 3D XY model ($\beta = 0.345$ and $\gamma = 1.316$), and tricritical mean-field model ($\beta = 0.25$ and $\gamma = 1$), the relation between $(M_s)^{1/\beta}$ and $(H/M)^{1/\gamma}$ can be established (known as the modified Arrott plot (MAP)). We further define the relative slopes $\text{RS} = S(T)/S(T_C)$, where $S(T)$ is the slope of $(M_s)^{1/\beta}$ vs.

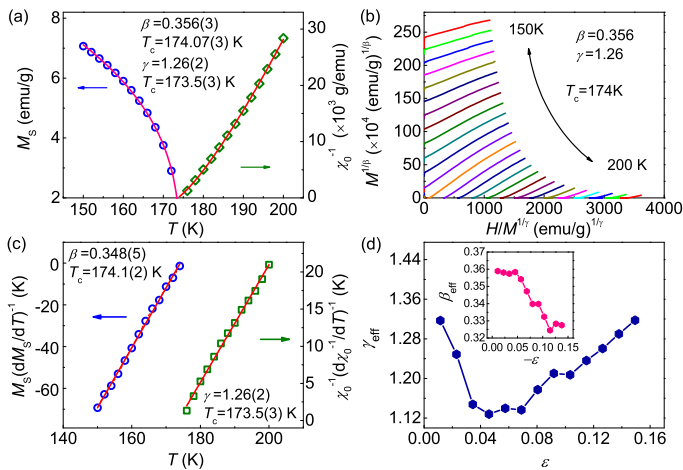


FIG. 3. (a) Temperature dependence of the spontaneous magnetization M_s (left) and the inverse initial susceptibility χ_0^{-1} (right) with solid fitting curves. (b) Modified Arrott plot isotherms $(H/M)^{1/\gamma}$ vs. $(M_s)^{1/\beta}$ with $\beta = 0.356$ and $\gamma = 1.26$. (c) The Kouvel-Fisher plot for the temperature dependence of the spontaneous magnetization M_s and (left) and the inverse initial susceptibility χ_0^{-1} (right) with solid fitting curves. (d) Effective exponents β_{eff} (inset) and γ_{eff} as a function of reduced temperature ε .

$(H/M)^{1/\gamma}$ at T . This parameter is a useful method to detect the validity of the MAP.^{30,31} In an ideal model, the proper choice critical exponents will produce a MAP with a series of parallel straight lines in the high-field region, so the value of RS should equal to 1. As shown in the inset of Fig. 2(b), the deviation of tricritical mean-field model is largest and other models also can not lead to the parallel linear relation between $(M_s)^{1/\beta}$ and $(H/M)^{1/\gamma}$. It clearly indicates that the critical behavior of $\text{Co}_3\text{Sn}_2\text{S}_2$ could not be described by these universality classes. Thus, the iteration method²⁹ with the initial trial values $\beta (= 0.325)$ and $\gamma (= 1.24)$ is used to extract the correct critical exponents. Briefly speaking, linear extrapolation of high-field straight line portion of the isotherm gives the value of $M_s(T)$ and $\chi_0^{-1}(T)$ as an intercepts on the $(M_s)^{1/\beta}$ and $(H/M)^{1/\gamma}$ axes, respectively. Use these values of $M_s(T)$ and $\chi_0^{-1}(T)$, we can get a new set of β and γ values by Eqs.(1) and (2) and then construct a new MAP. This procedure was repeated until the values stable. The converging values of β and γ obtained from the good fits of $M_s(T)$ and $\chi_0^{-1}(T)$ as a function of temperature are 0.356(3) and 1.26(2)(Fig. 3(a)), which are different from those exponents in above models. The fitted T_C s are also close to that derived from the $M(T)$ curve (inset of Fig. 1(b)). On the other hand, as shown in Fig. 3(b), it is obvious that all curves in MAP are straight lines and parallel to each other with the line at T_C just passing through the origin.

Alternatively, the critical exponents can also be deter-

mined by the Kouvel-Fisher (KF) method,³²

$$\frac{M_s(T)}{dM_s(T)/dT} = \frac{(T - T_C)}{\beta} \quad (3)$$

$$\frac{\chi_0^{-1}(T)}{d\chi_0^{-1}(T)/dT} = \frac{(T - T_C)}{\gamma} \quad (4)$$

According to Eqs. (3) and (4), plots of $M_s(T)/dM_s(T)/dT$ and $\chi_0^{-1}(T)/d\chi_0^{-1}(T)/dT$ against T yield linear curves with slopes of $1/\beta$ and $1/\gamma$, respectively, on which the intercepts on the abscissa axis are corresponding to T_C s. The critical exponents obtained from the KF method are $\beta = 0.358(5)$ with $T_C = 174.4(2)$ K and $\gamma = 1.311(2)$ with $T_C = 173.7(1)$ K (Fig. 3(c)), consistent with those derived from the MAP. On the other hand, temperature-dependent effective exponents β_{eff} and γ_{eff} in the asymptotic regime ($\varepsilon \rightarrow 0$) could reflect the existence of several competing couplings and/or disorder.³⁶ Both of them are defined as,

$$\beta_{eff}(\varepsilon) = \frac{d[\ln M_s(\varepsilon)]}{d(\ln |\varepsilon|)}; \gamma_{eff}(\varepsilon) = \frac{d[\ln \chi_0^{-1}(\varepsilon)]}{d(\ln \varepsilon)} \quad (5)$$

The β_{eff} and γ_{eff} as a function of reduced temperature ε are plot in Fig. 3(d). The β_{eff} almost changes monotonically with ε , while the γ_{eff} shows a nonmonotonic evolution with ε , indicating that the β_{eff} and γ_{eff} do not match any predicted universality class even in the asymptotic region. Similar phenomenon was reported in partially frustrated alloys, where the nonmonotonic changes were attributed to existence of magnetic disorders.^{7,37} But because the critical exponents of a magnet should be independent of the microscopic details of the system due to the divergence of the correlation length in the vicinity of the second-order phase transition, and the effective exponents are nonuniversal properties, the static critical exponents obtained from the MAP and KF method should be intrinsic.

The critical exponent δ is associated with the magnetization isotherm at T_C by the relationship $M = DH^{1/\delta}$, where D is the critical amplitudes.³² It can be obtained from the fitting of high-field slope of the $\log(M)$ vs. $\log(H)$ isotherms plot at T_C . Fig. 4 depicts the isotherm at 174 K, and the inset displays the plot on the log-log scale. The linear part in the high-field region gives the δ value of 4.52(4). In addition, the critical exponents from the static scaling analysis are related to the Widom scaling relation, $\delta = 1 + \gamma/\beta$.³³ Using the estimated values of β and γ from the MAP and the KF method yield $\delta = 4.662$ and 4.631, respectively, close to above value of δ . This, therefore, confirms that the critical exponents obtained by the magnetization data are reliable and in agreement with the scaling hypothesis. Furthermore, there is an important criterion for the critical regime based on the prediction of scaling hypothesis,³³

$$M(H, \varepsilon) = \varepsilon^\beta f_\pm(H/\varepsilon^{\beta+\gamma}) \quad (6)$$

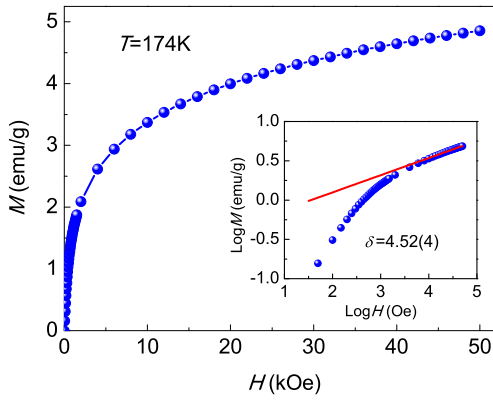


FIG. 4. Isothermal M-H plot at $T_c = 174$ K. Inset: same plot in log-log scale with the solid linear fitting.

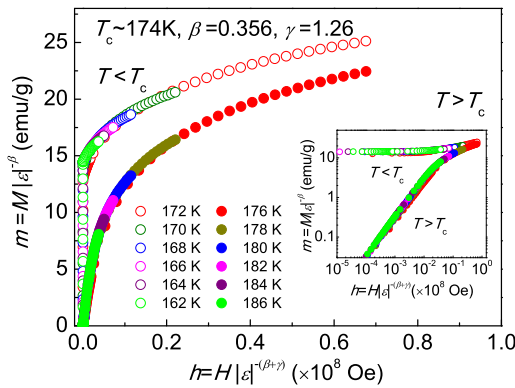


FIG. 5. Scaling plots below and above T_c using β and γ determined from the KF method. Inset: same plot in log-log scale.

where the functions f_+ for $T > T_C$ and f_- for $T < T_C$, respectively, are the regular functions. Based on the reasonable values of β and γ , the $M|\epsilon|^{-\beta}$ as a function of $H|\epsilon|^{-\beta+\gamma}$ plots in the critical region should fall onto two universal curves: one above T_C and another below T_C . The plot of $M|\epsilon|^{-\beta}$ against $H|\epsilon|^{-\beta+\gamma}$ close to the critical region is selectively depicted in Fig. 5 with the values of β and γ obtained from the KF method. Logarithmic scaled m vs. scaled h has been plotted in the inset for better clarity. It can be clearly seen that all of data fall onto two universal curves, verifying the critical behavior over the measured temperature range and hence ensuring the accuracy of critical exponents.

According to the normalization group analysis of exchange-interaction systems the universality class of the magnetic phase transition depends on the exchange distance $J(r)$. The long-range exchange interaction decays as $J(r) \sim r^{-(d+\sigma)}$ when the short-range exchange interaction decays as $J(r) \sim e^{-r/b}$, where σ is the range of the interaction, r is the distance, d is the dimensionality, and b is the spatial scaling factor.³⁸ Both of these spin interactions depends on the parameter of σ , that can be calculated by the equation,^{35,37,38}

TABLE I. Comparison of Critical exponents of $\text{Co}_3\text{Sn}_2\text{S}_2$ with different sets of $\{d : n\}$.

Critical exponents	$d = 3$ $n = 1$	$d = 3$ $n = 2$	$d = 3$ $n = 3$	$d = 2$ $n = 1$	$d = 2$ $n = 2$	$d = 2$ $n = 3$
σ	1.9276	1.8609	1.8215	1.2758	1.2336	1.2080
α	0.0389	-0.0312	-0.0752	0.0248	-0.0425	-0.0848
β	0.3505	0.3856	0.4076	0.3575	0.3913	0.4124
δ	4.5947	4.2674	4.0911	4.5238	4.2201	4.0553

$$\gamma = 1 + \frac{4n+2}{dn+8}\Delta\sigma +$$

$$\frac{8(n+2)(n-4)}{d^2(n+8)^2} \times \left[1 + \frac{2G(\frac{d}{2})(7n+20)}{(n-4)(n+8)}\right]\Delta\sigma^2 \quad (7)$$

where n is the spin dimensionality, $\Delta\sigma = \sigma - \frac{d}{2}$, $G(\frac{d}{2}) = 3 - \frac{1}{4}(\frac{d}{2})^2$. Based on this equation, $\sigma < 2$ indicates long range of spin interaction, while $\sigma > 2$ indicates the short range of spin interaction. Since the experimental value of γ is 1.26, with any combination of $\{d : n\}$ the values of σ are always smaller than 2, indicating that the theoretically predicted 3D short-range type could not support the exchange interactions in $\text{Co}_3\text{Sn}_2\text{S}_2$ spin systems. To the present case, the σ value should be determined by the isotropic long-range exchange interactions of the form $J(r) \sim r^{-(d+\sigma)}$. The remaining exponents can be calculated from the following expressions: $\nu = \gamma/\sigma$, $\alpha = 2 - \nu d$, $\beta = (2 - \alpha - \gamma)/2$, $\delta = 1 + \gamma/\beta$. Using the experimental value of γ , other critical exponents for different sets of $\{d : n\}$ are calculated and listed in Table 1 for comparison. The calculated exponents do not match well with any of the 3D models and the presently determined values of $\beta = 0.356(3)$ and $\delta = 4.52(4)$ match those calculated values for a $d = 2$ and $n = 1$ ferromagnet with a long-range interaction between the spins decaying with distance as $J(r) \sim r^{-3.28}$. It implies that the asymptotic critical behavior of $\text{Co}_3\text{Sn}_2\text{S}_2$ corresponds to spin system with space and spin dimensionality of $d = 2$ and $n = 1$. Similar phenomenon has also been observed in various other itinerant magnetic systems, such as $\text{Pr}_{0.5}\text{Sr}_{0.5}\text{MnO}_3$, Cr-Fe alloy, Y_2Ni_7 systems.^{9,37,38} Moreover, it is also consistent with layered structure of $\text{Co}_3\text{Sn}_2\text{S}_2$ in which the easy-axis is along the c axis with small saturated moment ($\sim 0.3 \mu_B/\text{Co}$).²⁰

IV. CONCLUSION

In summary, the critical exponents are comprehensively investigated in the vicinity of the PM-FM transition in HFM $\text{Co}_3\text{Sn}_2\text{S}_2$. This transition is found to be a second-order phase transition. The critical exponents obtained from various techniques are consistent with each other, and the experimentally obtained isothermal mag-

netization curves measured at different temperature collapses into two universal branches below and above T_C . It confirms that the obtained exponents are intrinsic feature of transition in $\text{Co}_3\text{Sn}_2\text{S}_2$. Further analysis suggests that the exchange interaction is long-range, decaying with distance as $J(r) \sim 1/r^{-3.28}$, and the space and spin dimensionalities are $d = 2$ and $n = 1$, respectively. These critical behaviors agree well with the weak itinerant character of layered HMF $\text{Co}_3\text{Sn}_2\text{S}_2$.

V. ACKNOWLEDGMENTS

This work was supported by the Ministry of Science and Technology of China (No. 2016YFA0300504); the National Natural Science Foundation of China (No. 11574394, 11774423); the Research Funds of Renmin University of China (RUC) (No. 15XNLF06, 15XNLQ07); the Fundamental Research Funds for the Central Universities (No. 2017RC20, 2017RC02); and the Research Innovation Fund for College Students of Beijing University of Posts and Telecommunications.

-
- ¹ S. L. Sondhi, S. M. Girvin, J. P. Carini, and D. Shahar, *Rev. Mod. Phys.* **69**, 315 (1997).
- ² J. Lin, P. Tong, D. Cui, C. Yang, J. Yang, S. Lin, B. Wang, W. Tong, L. Zhang, Y. Zou, and Y. Sun, *Sci. Rep.* **5**, 7933 (1997).
- ³ L. Zhang, B. Wang, Y. Sun, P. Tong, J. Fan, C. Zhang, L. Pi, and Y. Zhang, *Phys. Rev. B* **85**, 104419 (2012)
- ⁴ B. S. Wang, C. C. Li, S. Lin, J. C. Lin, L. J. Li, P. Tong, W. J. Lu, X. B. Zhu, Z. R. Yang, and W. H. Song, *J. Mag. Mater.* **323**, 2017 (2011).
- ⁵ J. S. Kouvel and J. B. Cowly, *Critical Phenomena in Alloys, Magnets and Superconductors*, edited by R. E. Mills, E. Ascher, and R. I. Jaffee, McGraw-Hill, New York (1971).
- ⁶ O. Boxberg and K. Westerholt, *Phys. Rev. B* **50**, 9331 (1994).
- ⁷ A. Perumal and V. Srinivas, *Phys. Rev. B* **67**, 094418 (2003).
- ⁸ A. Semwal and S. N. Kaul, *Phys. Rev. B* **64**, 014417 (2001).
- ⁹ A. Bhattacharyya, D. Jain, V. Ganesan, S. Giri, and S. Majumdar, *Phys. Rev. B* **84**, 184414 (2011)
- ¹⁰ M. Shimizu, *Rep. Prog. Phys.* **44**, 330 (1981).
- ¹¹ T. Moriya and Y. Takahashi, *Ann. Rev. Mater. Sci.* **14** 1 (1984).
- ¹² T. Moriya, *Spin Fluctuations in Itinerant Electron Magnetism*, Springer, Berlin (1985).
- ¹³ R. A. de Groot, F. M. Mueller, P. G. van Engen, and K. H. J. Buschow, *Phys. Rev. Lett.* **50**, 2024-2027 (1983).
- ¹⁴ R. C. O'Handley, *Modern Magnetic Materials*, Wiley, New York (2000).
- ¹⁵ J. M. D. Coey and M. Venkatesan, *J. Appl. Phys.* **91**, 8345 (2002).
- ¹⁶ K. I. Kobayashi, T. Kimura, H. Sawada, K. Terakura, and Y. Tokura, *Nature* **395**, 677 (1998).
- ¹⁷ J. S. Moodera and G. Mathon, *J. Mag. Mater.* **200**, 248 (1999).
- ¹⁸ I. Žutić, J. Fabian, and S. Das Sarma, *Rev. Mod. Phys.* **76**, 323 (2004).
- ¹⁹ R. Weihrich, A. C. Stckl, M. Zabel, and W. Schnelle, *Z. Anorg. Allg. Chem.* **630**, 1767 (2004).
- ²⁰ W. Schnelle, A. Leithe-Jasper, H. Rosner, F. M. Schapacher, R. Pottgen, F. Pielhofer, and R. Weihrich, *Phys. Rev. B* **88**, 144404 (2013).
- ²¹ Q. Wang, Y. F. Xu, R. Lou, Z. H. Liu, M. Li, Y. B. Huang, D. W. Shen, H. M. Weng, S. C. Wang, and H. C. Lei, arXiv: 1712.09947 (2017).
- ²² E. Liu, Y. Sun, L. MÜchler, A. Sun, L. Jiao, J. Kroder, V. Süß, H. Borrmann, W. Wang, W. Schnelle, S. Wirth, S. T. B. Goennenwein, and C. Felser, arXiv: 1712.06722 (2017).
- ²³ J. Y. Fan, L. S. Ling, B. Hong, L. Zhang, L. Pi, and Y. H. Zhang, *Phys. Rev. B* **81**, 144426 (2010).
- ²⁴ K. Ghosh, C. J. Lobb, R. L. Greene, S. G. Karabashev, D. A. Shulyatev, A. A. Arsenov, and Y. Mukovskii, *Phys. Rev. Lett.* **81**, 4740 (1998).
- ²⁵ M. A. Kassem, Y. Tabata, T. Waki, and H. Nakamura, *J. Cryst. Growth* **426**, 208 (2015).
- ²⁶ TOPAS Version 4.2, Bruker AXS, Karlsruhe, Germany (2009).
- ²⁷ A. Umetani, E. Nagoshi, T. Kubodera, and M. Matoba, *Physica B* **403**, 1356 (2008).
- ²⁸ S. K. Banerjee, *Phys. Lett.* **12**, 16 (1964).
- ²⁹ M. H. Phan, G. T. Woods, A. Chaturvedi, S. Stefanoski, G. S. Nolas, and H. Srikanth, *Appl. Phys. Lett.* **93**, 252505 (2008).
- ³⁰ S. Mahjoub, M. Baazaoui, R. Mnassri, N. Boudjada, and M. Oumezzine, *J. Alloys Comp.* **633**, 207 (2015).
- ³¹ R. Mnassri, N. Chniba-Boudjada, and A. Cheikhrouhou, *J. Alloys Comp.* **640**, 183 (2015).
- ³² J. S. Kouvel and M. E. Fisher, *Phys. Rev. A* **136**, A162616 (1964).
- ³³ B. Widom, *J. Chem. Phys.* **43**, 3898(1965).
- ³⁴ K. Huang, *Statistical Mechanics*, 2nd ed. (Wiley, New York, 1987).
- ³⁵ M. E. Fisher, S.-k. Ma, and B. G. Nickel, *Phys. Rev. Lett.* **29**, 917 (1972).
- ³⁶ A. Perumal, V. Srinivas, V. V. Rao, and R. A. Dunlap, *Phys. Rev. Lett.* **91**, 137202 (2003).
- ³⁷ A. K. Pramanik and A. Banerjee, *Phys. Rev. B* **79**, 214426 (2009).
- ³⁸ S. F. Fischer, S. N. Kaul, and H. Kronmüller, *Phys. Rev. B* **65**, 064443 (2002).